Design of a thick-walled screen for flow equalization in microstructured reactors

Please check the document version of this publication:

• A submitted manuscript is the version of the article upon submission and before peer-review. There can be important differences between the submitted version and the official published version of record. People interested in the research are advised to contact the author for the final version of the publication, or visit the DOI to the publisher's website.
• The final author version and the galley proof are versions of the publication after peer review.
• The final published version features the final layout of the paper including the volume, issue and page numbers.

Link to publication

Design of a thick-walled screen for flow equalization in microstructured reactors

Evgeny V Rebrov, Rahul P Ekatpure, Mart H J M de Croon and Jaap C Schouten[1]

Laboratory of Chemical Reactor Engineering, Eindhoven University of Technology,
PO Box 513, 5600 MB Eindhoven, The Netherlands

E-mail: j.c.schouten@tue.nl

Abstract

A systematic computational fluid dynamics (CFD) approach has been applied to design the geometry of the channels of a three-dimensional (thick-walled) screen comprising upstream and downstream sets of elongated channels positioned at an angle of 90° with respect to each other. Such a geometry of the thick-wall screen can effectively drop the ratio of the maximum flow velocity to mean flow velocity below 1.005 in a downstream microstructured reactor at low Reynolds numbers. In this approach the problem of flow equalization reduces to that of flow equalization in the first and second downstream channels of the thick-walled screen. In turn, this requires flow equalization in the corresponding cross-sections of the upstream channels. The validity of the proposed design method was assessed through a case study. The effect of different design parameters on the flow non-uniformity in the downstream channels has been established. The design equation is proposed to calculate the optimum values of the screen parameters. The CFD results on flow distribution were experimentally validated by Laser Doppler Anemometry measurements in the range of Reynolds numbers from 6 to 113. The measured flow non-uniformity in the separate reactor channels was below 2%.

(Some figures in this article are in colour only in the electronic version)

Introduction

The flow non-uniformity in a microstructured reactor can be divided into gross and channel-to-channel non-uniformity [1]. The latter is caused by manufacturing tolerances [2], the differences in the thickness of catalytic layers and the local temperature differences in the microchannels, which change the physical properties of the fluid [3]. However, usually such differences do not exceed 5%. On the other hand, the gross flow non-uniformity is mainly associated with the poor design of the header configuration, or with the improper choice of the drag coefficient of the flow distributor. Especially at low *Re* numbers (0.5–5), which are often observed in microreactors, the ratio of the maximum flow velocity to the minimum flow velocity in different channels can be as high as 2. It has to be mentioned that there is a clear difference between planar

(or thin-walled) and three-dimensional (thick-walled) screens. The former does not have guiding walls while the latter consists of a number of thick bars, whose thickness in the direction of the fluid flow equals or exceeds the spacing between them. A planar screen cannot ensure a uniform velocity distribution when the ratio of open cross-section of the screen is by an order of magnitude larger than that of the inlet pipe [4, 5], which is a common case in microreaction technology. The application of planar screens can even amplify their flow non-uniformity downstream, giving to the flow profile a distribution, which is directly opposite to that of the distribution upstream of the screen. This problem does not exist in the case of thick-walled screens, as the degree of velocity equalization is virtually the same at all cross-sections downstream from them [6].

The literature on the design of the geometry of either an upstream (diffuser) or downstream (confuser) thick-walled screen for different structured applications is scarce. An outlet

---

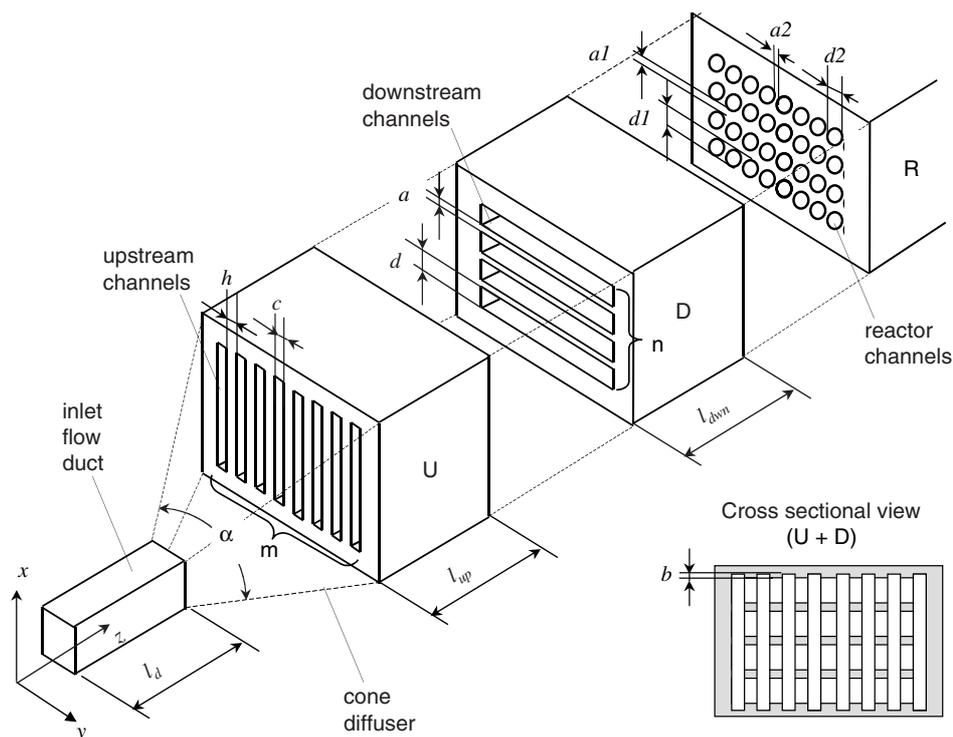[1] Author to whom any correspondence should be addressed.

Figure 1. The header consists of a cone diffuser and a thick-walled screen positioned in front of the microreactor. The thick-walled screen consists of two sections positioned with a 90° turn relative to each other. The upstream section (U) comprises a set of *m* elongated parallel upstream channels, and the downstream section (D) comprises a set of *n* elongated parallel downstream channels positioned at an angle of 90° with respect to the upstream channels. Parameter *a* is the minimum length between two neighboring downstream channels, parameter *b* is the distance in cross-sectional view between a top wall of the first downstream channel and a side wall of the upstream channels. Parameter *c* is the width of the upstream channels. Parameter *d* is the height of the downstream channels. Parameter *h* is the distance between the neighboring upstream channels. Parameters l_{up} and l_{dwn} are the lengths of upstream and downstream channels of the screen, respectively. Parameters *a*1 and *a*2 are the distances in the *x*- and *y*-directions, respectively, between the channels of the microreactor (R) connected to the downstream channels of the header. Parameters *d*1 and *d*2 are the dimensions of the reactor channels in the *x*- and *y*-directions, respectively. *d*1 is usually equal to or slightly lower than distance *d*, so the distance in the vertical direction between the channels in the microreactor (*a*1) is equal to or slightly higher than distance *a*.

diffuser system consisting of capillary elements, which can be regarded as thick-wall screens, is described in [7]. This system is used for improving the performance of combustion engines. Another geometry comprising a thick-walled screen is proposed for distributing the fluid flow from one flow cross-section to a different flow cross-section in a funnel-shaped tubular header [8]. In this header, a plate having a multiplicity of parallel passages is arranged perpendicular to the axis of the tubular header leaving free passage openings between the edge of the plate and the tubular header. The flared opening of the funnel-shaped tubular header is filled by an end plate with a multiplicity of parallel passage channels. An interfacial surface generator with mixing baffles (thin-walled screens) placed in a pipe can be applied [9]. In this design, the fluid stream is divided and recombined into flow passages which have an elongated cross-section. Another flow distributor, which consists of three functionally distinct sub-elements, is described in [10]. The first sub-element divides a fluid stream into branch streams. Then, the second sub-element expands the branch streams. Finally, the third sub-element performs the functions of contracting the branch streams, independently adjusting their flow rates and recombining them into an integrated whole. A feature of common significance is the symmetrical expansion and contraction of the divided and

stacked branch streams. Two recent papers are related to the improvement of the performance of plate-fin heat exchangers operating in the turbulent mode [11, 12]. The authors studied the fluid flow maldistribution using computational fluid dynamics (CFD) simulations. Especially, the effects of the configuration of header and distributor on the flow distribution have been investigated. Numerical investigation showed that application of a two-stage distribution structure improved the flow distribution for plate-fin heat exchangers [12].

Recently, we proposed a header consisting of a flow diffuser and a thick-walled screen consisting of upstream and downstream parallel channels for flow equalization over the cross-section of a microstructured reactor [6, 13]. The upstream section (U) comprises a set of *m* elongated parallel upstream channels, and the downstream section (D) comprises a set of *n* elongated parallel downstream channels positioned at an angle of 90° with respect to the upstream channels (figure 1). In the present geometry, parameter *a* is the distance between two neighboring downstream channels, and parameter *b* is the distance in cross-sectional view between a top wall of the first downstream channel and a side wall of the upstream channels. In other words, the value *b* is the overhang of the cross-section of upstream channels with respect to the cross-section of the first downstream channel. Parameter *c* is the

width of the upstream channel. Parameter d is the height of the downstream channel. Parameter h is the distance between the neighboring upstream channels. Parameters l_{up} and l_{dwn} are the lengths of upstream and downstream channels of the screen respectively. $d1$ is the diameter of the channels in the microreactor (R) connected to the downstream channels of the header. $d1$ is usually equal to or slightly lower than parameter d, so the distance in the vertical direction between the channels in the microreactor ($a1$) is equal to or slightly higher than distance a.

Comparing to the applications mentioned above [7–11] the present configuration of the header is intended for operation in laminar mode with low Re numbers ($Re < 10$) resulting in a negligible pressure drop across the reactor. A CFD analysis was performed on this type of header [14]. The geometry of the inlet section allows us to obtain a highly uniform distribution of fluid flow at the end face of the inlet section (or to the inlet face of a downstream reactor), regardless of the fluid flow distribution profile at the inlet face of the upstream channels [6]. The approach for flow equalization in a downstream microreactor was presented by the application of a thick-wall screen, in which parameter b was adjusted in a way that function f, given by equation (1), has to be equal to unity [6]:

$$f = \frac{(a + 2b + 2d)^4}{(a + 2b + c + 2d)^2 (2a + 2d)^2} \frac{Po_{V2}}{Po_{V1}}. \tag{1}$$

The Poiseuille number [15] is

$$Po(t, x^+) = \frac{3.44}{\sqrt{x^+}}$$
$$+ \frac{\frac{0.674 + 1.3061t + 0.1222t^2 - 0.6718t^3}{4x^+} + 24P(t) - \frac{3.44}{\sqrt{x^+}}}{1 + \frac{2.9 \times 10^{-5} + 7.0 \times 10^{-5}t + 9.7 \times 10^{-4}t^2 - 7.8 \times 10^{-4}t^3}{(x^+)^2}} \tag{2}$$

where $P(t) = 1 - 1.3553t + 1.9467t^2 - 1.7012t^3 + 0.9564t^4 - 0.2537t^5$, with t being the aspect ratio, i.e. $t = \frac{c}{a + 2(b+d)}$. $x_{up}^+ = \frac{l_{up}}{D_h Re}$ is the dimensionless length of the upstream channel, l_{up} is the length of upstream channels, $Re = \frac{\overline{v} \rho D_h}{\eta}$ is the Reynolds number, $\overline{v} = \frac{1}{A} \int_A v \, dA$ is the average velocity over cross-section A of a fluid channel, η is the fluid viscosity and $D_h = \frac{4A}{P}$ is the hydraulic diameter. For the screen applied: $z_{V1} = a + 2b + 2d$, $z_{V2} = 2(a + d)$.

In this approach the problem of flow equalization reduces to that of flow equalization in the first and second downstream channels of the thick-walled screen. In turn, this requires flow equalization in the corresponding cross-sections of the upstream channels (figure 2(a)), which have been modeled by rectangular and parallel plate geometries. In this way, the hydraulic conductance and the corresponding Po numbers were calculated for a rectangle with height z_{V1} obtained by the topmost and bottommost portion of upstream channels merged together (figure 2(b)), and for the middle part which was considered as parallel plates with height z_{V2} (figure 2(c)) [6]. The results of the CFD simulations were verified by measuring flow distribution at the outlets of the downstream channels by Laser Doppler Anemometry (LDA) as described elsewhere [16]. The experimental results showed good agreement with numerical results for a wide range of Re numbers. It was found that parameter b governs the flow behavior at the interface between the upstream and downstream channels of
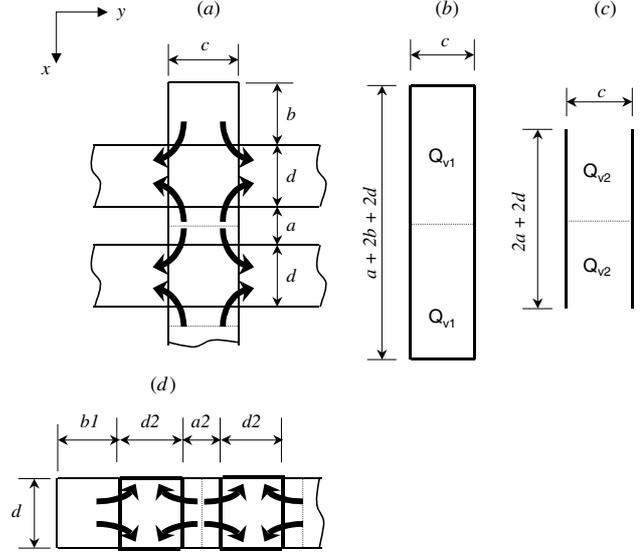

Figure 2. Decomposition of the upstream channel geometry (a) into regular pieces: (b) two half rectangles merged together and (c) parallel plates. (d) The geometry of the interface between the downstream section (D) and the microstructured reactor (R). See figure 1 for parameter definitions.

the screen and is responsible for uniform flow distribution. Depending on the design parameters, there exists an optimum value of parameter b, which provides the minimum flow non-uniformity below 0.2%. The approach has been successfully applied in the design of a header for uniform flow distribution in a downstream microstructured reactor [16–18].

In this work, a design equation is proposed to calculate the optimum value of parameter b, as a function of design parameters a, c, d and the dimensionless length of the upstream channels (x_{up}^+), which gives minimum flow non-uniformity in the downstream microstructured reactor. The results obtained using design equation (1) are validated by CFD analysis. The conclusions of this paper are of great significance on the improvement and optimum design of thick-walled screens applied at the upstream of the microstructured reactors for flow equalization.

Parametric study by the mathematical model of a thick-walled screen

Effect of parameter a

As parameter a increases, the b/a ratio has to be reduced to obtain flow equalization in the whole range of values of parameter a [6, 14]. Therefore, the problem can be formulated as finding an optimum fit, which minimizes the flow non-uniformity index Ω defined as

$$\Omega = \left[\frac{1}{a_2 - a_1} \int_{a_1}^{a_2} f(a, b, c, d, x_{up}^+) \, da \right] - 1 \tag{3}$$

where function f is defined by equation (1). The index Ω is the average value of the function f on the interval of values a between $a_1 = 100 \, \mu$m and $a_2 = 1000 \, \mu$m, which are of interest for microreactor applications. Several functions with two fitting parameters can be used to describe the ensemble of data
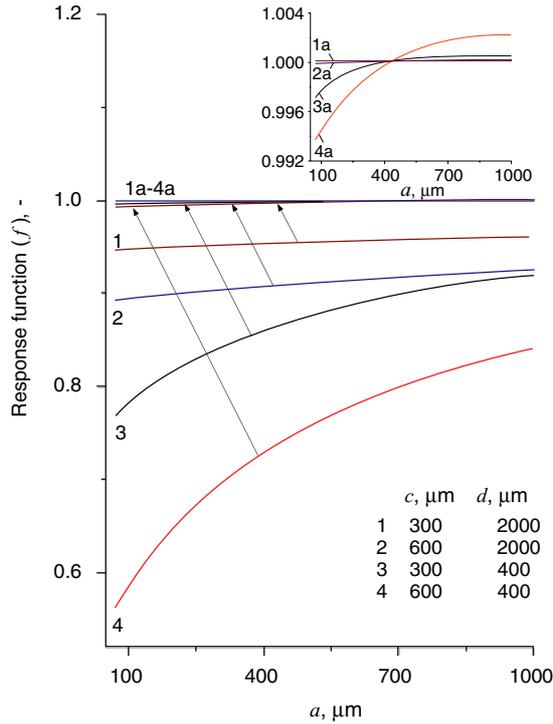
Figure 3. Response function *f* as a function of distance between the downstream channels: curves 1–4 are obtained at $b/a = 0.5$. Curves 1a–4a are obtained with the fitting function given by equation (6).

points generated by the screen model. In their discrimination, the following criteria were applied:

$$\Omega \leqslant 1 \times 10^{-5} \tag{4}$$

$$\left| f\left(a, b, c, d, x_{\text{up}}^{+}\right) - 1 \right| \leqslant 0.005$$
$$\text{for} \quad 100 \leqslant a \leqslant 1000 \, (\mu\text{m}). \tag{5}$$

The first criterion is set to minimize the flow non-uniformity in the whole range of values of parameter *a*. The second criterion states that at any given value of parameter *a*, the flow non-uniformity should not exceed 0.5%. To satisfy the constraints given by equations (4) and (5), a fitting function for the *b/a* ratio can be found in the form

$$\frac{b}{a} = P1 + \frac{P2}{a}. \tag{6}$$

Figure 3 demonstrates two sets of *f*-function plots, one at the constant *b/a* ratio of 0.5 and the other when the fitting function given by equation (6) was applied. It can be seen that flow equipartition is achieved in the whole range of *a*-values for different values of parameters *c* and *d* if the *b/a* ratio is a function of the parameter *a*, and the fitting parameters *P1* and *P2* are properly chosen (see table 1). It can be seen from table 1 that parameter *P1* is always 0.5, while parameter *P2* depends on parameters *c* and, to a lesser extent, on parameter *d*. Therefore, the fitting function can be rewritten as follows:

$$b(a, c, d) = 0.5a + P2(c, d). \tag{7}$$

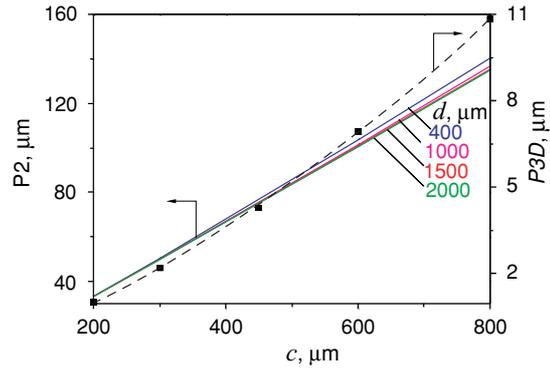Thus, it is necessary to establish the dependence of parameter *P2* on design variables *c, d* and x_{up}^{+}.

Figure 4. Parameters *P2* and *P3D* as a function of the width of the upstream channels.

Table 1. Fitting parameters *P1* and *P2* for the parameter *b*: $b(a) = P1 \cdot a + P2$. The dimensionless length of the upstream channels equals 0.9.

c (μm)	d (μm)	$P1$ (–)	$P2$ (μm)
300	400	0.500	57.00
300	2000	0.500	56.65
600	400	0.500	115.8
600	2000	0.500	113.4

Effect of parameters c and d

Initially, parameter x_{up}^{+} was fixed at 5.0, corresponding to a fully developed flow in the upstream channels, and the values of parameter *P2*, satisfying the criteria 4 and 5, were calculated for a wide range of values of design parameters *c* and *d*: 200–800 and 200–2000 μm, respectively. In these calculations, the functional dependence of *b(a)* according to equation (7) was applied to reach flow equipartition in the whole range of values of parameter *a* of 100–1000 μm. Figure 4 shows *P2* values as a function of the width of the upstream channels (*c*). When the *d/c* ratio becomes larger than 5, a linear increase of parameter *P2* with increasing parameter *c* is observed. Based on these observations, the following fitting function for parameter *P2* was chosen:

$$P2(c, d) = P2A + P2Bc + P3(c, d). \tag{8}$$

The slope of the curves (*P2B*) remains constant ($0.167\,80 \pm 0.000\,05$) when the *d/c* ratio exceeds 5, whereas it slightly increases with decreasing *d/c* ratio. A new parameter (*P3*) is introduced to describe the deviation of *P2* from a linear behavior at low *d/c* ratios. When the values generated by the screen model were fitted using equation (8) over the entire range of parameters *c* and *d*, it was found that the *y*-intercept (*P2A*) was always 0.0 ± 0.1 μm. Therefore, equation (8) can be rewritten as

$$P2(c, d) = 0.1678c + P3. \tag{9}$$

Dividing both sides of equation (9) by $0.1678c$, we have

$$\frac{P2}{0.1678c} - 1 = \frac{P3}{0.1678c}. \tag{10}$$

Figure 5 shows the plots of $\frac{P2}{0.1678c} - 1$ as a function of the height of downstream channels (*d*) at several different values of the width of the upstream channels (*c*). It can be seen that
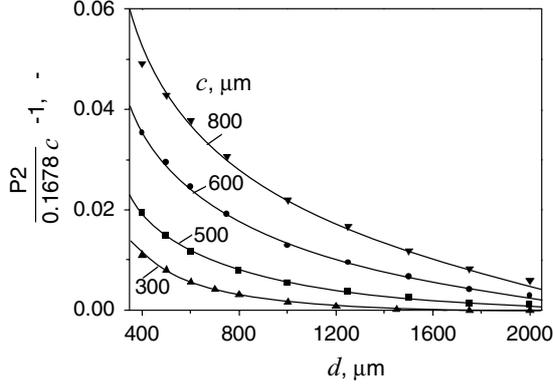
Figure 5. Parameter $\frac{P2}{0.1678c} - 1$ as a function of the height of the downstream channels, at different values of the width of the upstream channel, namely 300, 500, 600 and 800 μm.
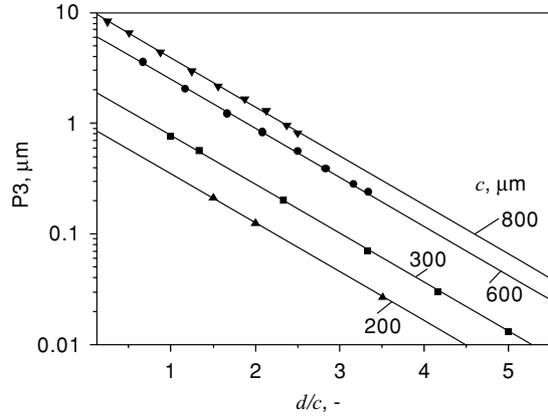

Figure 6. Parameter $P3$ as a function of the ratio of the height of the downstream channels to the width of the upstream channels.

at a small value of parameter c of 300 μm, the $P3$ contribution approaches zero already at $d = 1500$ μm. At a larger value of parameter c of 500 μm, this happens at $d = 2500$ μm (not shown in figure 5). As parameter c increases, the minimum value of parameter d, above which the contribution of $P3$ to $P2$ (see equation (9)) can be neglected, becomes higher. However, the d/c ratio, beyond which the contribution of parameter $P3$ becomes negligible, remains constant and is approximately 5.

The values of $P3$ as a function of d/c ratio become less than 0.1 μm when $d/c > 5$ for the whole range of values of parameter c (figure 6). When the y-axis is plotted on the logarithmic scale versus d/c values, the symbols form straight lines for all values of parameter c and the slope of all curves is the same. This suggests that the fit for $P3$ has to be an exponential function over the entire range of d/c values:

$$P3(c, d) = P3D(c)\, e^{-P3E\frac{d}{c}}. \tag{11}$$

The fitting results give almost the same $P3E$ values of 1.020 ± 0.001 for different values of parameter c. Therefore, parameter $P3E$ was fixed and the dependence of $P3D$ on c was evaluated. The symbols in figure 4 represent the $P3D$ values as a function of parameter c. The values were fitted by a second-order polynomial function within 5% accuracy:

$$P3D(c) = P3A + P3Bc + P3Cc^2. \tag{12}$$
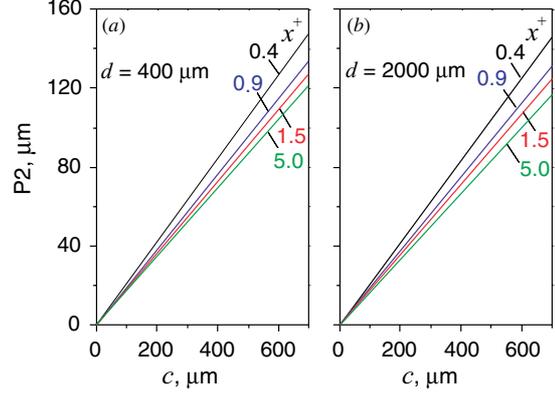
The fitting parameters are listed in table 2.

Figure 7. Parameter $P2$ as a function of the width of the upstream channels, at different dimensionless lengths of the upstream channels. The height of the downstream channels is (a) 400 μm, (b) 2000 μm.

Effect of the dimensionless length of the upstream channels (x_{up}^+)

So far, all calculations were carried out at x_{up}^+ values corresponding to a fully developed flow in the upstream channels ($x_{up}^+ > 5$). However, often a shorter length of the diffuser upstream section can provide an even flow distribution in the downstream channels. Thus, it is of particular interest to study the dependence of $P1$, $P2$ and $P3$ when parameter x_{up}^+ decreases. The low limit of x_{up}^+ values was set at 0.4, because beyond this value, the contribution from normal velocities to the overall velocity vector becomes substantial for the set of design parameters applied in this study. As a result, such a screen may not be considered as a thick-walled screen any longer.

Figure 7 shows that the dimensionless length x_{up}^+ is another important parameter affecting the flow distribution in a thick-wall screen. Parameter $P2$ increases with decreasing x_{up}^+. Therefore, as opposed to $P3$, the contribution of $P4$ is directly proportional to parameter c:

$$P2 = \left(0.1678 + P4(x_{up}^+)\right)c + P3(c, d). \tag{13}$$

Figure 8 demonstrates that the plots of $P4$ as a function of x_{up}^+ are located very close to each other and can be generally described by the same fitting function. It should be noted that at least three fitting parameters are required to get a good correlation between the fit and model prediction within a maximum error of 3%.

$$P4(x_{up}^+) = P4X\, \exp\left(P4E1 \cdot x_{up}^+ + \frac{P4E2}{x_{up}^+}\right). \tag{14}$$

In this fit, the parameters in the exponent do not depend on design parameters c and d. The regression analysis performed on four curves corresponding to the extreme values of design parameters c and d gives the values of $P4X = 0.035 \pm 0.001$, $P4E1 = -0.840 \pm 0.001$ and $P4E2 = 0.1986 \pm 0.004$. Using these values, the maximum deviations of the data obtained by the screen model from the correlation given by equation (14) are 2.7% for the $1.5 < x_{up}^+ < 3$ range and always below 1.5% for $0.4 < x_{up}^+ < 1.5$ and $x_{up}^+ > 3$.

Table 2. Fitting parameters for equations (6)–(14).

Parameter	Value	95% range	Fitting range
b	$P1Ba + P2$	–	$50 \leqslant a \leqslant 1000$ (μm)
$P1B$	0.500	$\pm 1.0 \times 10^{-3}$	
$P2$	$P2Bc + P3 + P4$	–	$200 \leqslant c \leqslant 800$ (μm)
$P2B$	0.1678	$\pm 5.0 \times 10^{-5}$	
$P3$	$P3D \exp(-P3E\frac{d}{c})$	–	$0.25 \leqslant \frac{d}{c} \leqslant 10$
$P3A$	-1.06	± 0.05	
$P3B$	8.47×10^{-3}	$\pm 0.08 \times 10^{-3}$	
$P3C$	8.00×10^{-6}	$\pm 0.07 \times 10^{-6}$	
$P3D$	$P3A + P3Bc + P3Cc^2$	–	$200 \leqslant c \leqslant 800$ (μm)
$P3E$	1.020	± 0.001	
$P4$	$P4X \exp(-0.840x^+ + 0.1986(x^+)^{-1})$	–	$x^+ \geqslant 0.4$
$P4X$	3.50×10^{-2}	$\pm 0.20 \times 10^{-2}$	$200 \leqslant c \leqslant 800$ (μm), $200 \leqslant d \leqslant 2000$ (μm)

Table 3. Comparison between values of parameter $P2$ obtained by the exact solution using a thick-wall screen model and the fitting function (equation (15)).

| x_{up}^+	d (μm)	Exact solution	Fit	Exact solution	Fit	Exact solution	Fit
		$c = 200$ μm		$c = 500$ μm		$c = 800$ μm	
0.4	200	42.24	42.12	106.15	107.89	168.48	175.51
	1000	42.08	41.78	105.55	105.12	169.64	170.14
	2000	42.06	41.78	105.27	104.53	168.79	167.96
1.5	200	36.21	36.17	92.77	93.01	149.93	151.70
	1000	35.87	35.83	90.38	90.24	146.25	146.33
	2000	35.85	35.83	89.83	89.65	144.43	144.15
5.0	200	33.90	34.01	87.50	87.61	142.58	143.07
	1000	33.56	33.68	84.59	84.85	137.18	137.20
	2000	33.55	33.67	84.01	84.26	135.16	135.20
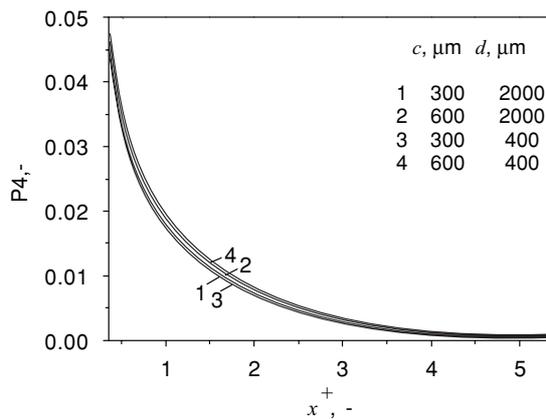
Figure 8. Parameter $P4$ as a function of the dimensionless length of the upstream channels at several different values of the width of the upstream channels and the height of the downstream channels.

Design equation

Summarizing equations (7) and (11)–(14), the design equation for a thick-walled screen can be obtained:

$$b(a, c, d, x_{up}^+) = 0.5a + 0.1678c$$

$$+ 0.035c \, \exp\left(-0.840x_{up}^+ + \frac{0.1986}{x_{up}^+}\right)$$

$$+ (-1.06 + 8.47 \times 10^{-3}c + 8.00 \times 10^{-6}c^2) \, e^{-1.02\frac{d}{c}}. \quad (15)$$

Table 3 gives an overview of the predictions of the fitting function given by equation (15) with the exact solutions derived from minimization of equation (3) at three different values of design parameters c, d and x_{up}^+. Table 4 presents the

Table 4. The relative difference (β (%) see equation (16)) between the results obtained by equation (13) with the exact solution given by equation (4).

x_{up}^+	d (μm)	$c = 200$ μm	$c = 500$ μm	$c = 800$ μm
0.4	200	-0.28	1.64	4.17
	1000	-0.71	-0.41	0.29
	2000	-0.67	-0.70	-0.49
1.5	200	-0.11	0.26	1.18
	1000	-0.11	-0.15	0.05
	2000	-0.06	-0.20	-0.19
5.0	200	0.32	0.13	0.34
	1000	0.36	0.31	0.01
	2000	0.36	0.30	0.03

relative difference in percent between the predictions obtained by the fitting function (equation (13)) and the exact solution for parameter $P2$ (equations (4), (5)):

$$\beta(\%) = \frac{P2(\text{Eq.}(13)) - P2(\text{Eq.}(4))}{P2(\text{Eq.}(4))} \times 100. \quad (16)$$

It can be seen that the fitting function describes well the whole range of design parameters with the only considerable deviation of 4.2% at $c = 200$ μm, $d = 200$ μm and $x_{up}^+ = 0.4$. Thus, it can be used for predictions of parameter $P2$ to design the upstream channels of a thick-walled screen.

CFD modeling of the thick-walled screen

The comparative CFD data were collected for a selected number of geometries of a thick-walled screen. In this work, the CFD code FLUENT® 6.0 was used to simulate the fluid flow distribution and pressure drops along the screens. The
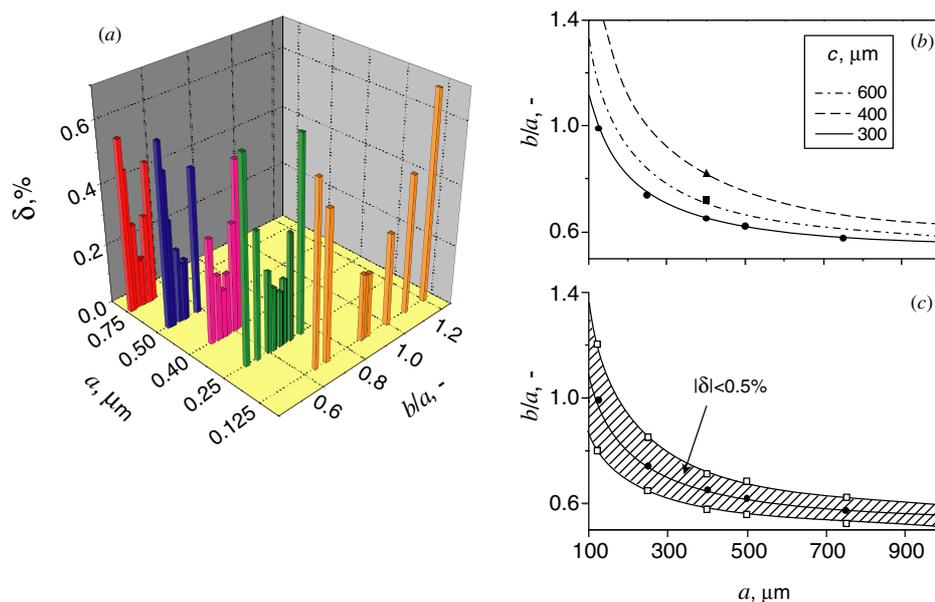
Figure 9. (*a*) Flow non-uniformity as a function of the distance between the downstream channels and the b/a ratio. (*b*) b/a ratios providing minimum flow non-uniformity as a function of the distance between the upstream channels, at different values of width of the upstream channel c, namely 300, 400 and 600 μm. The shaded area in (*c*) represents the range of b/a ratios where flow non-uniformity does not exceed 0.5% for $c = 300$ μm.

governing equations were the same as applied in [6]. The semi-implicit SIMPLER algorithm is used in the velocity and pressure conjugated problem. Boundary conditions applied are as follows: inlet fluid Reynolds numbers and outlet pressure are given, and no slip occurs at the wall. The convergence criterion is specified to residuals smaller than 1×10^{-6}. The header has two symmetry planes; hence, only one-fourth of the screen was modeled. The number of mesh elements was 20 000. A mesh independency check was performed on the results of the CFD model.

Figure 9(*a*) shows flow non-uniformity (δ) as a function of the b/a ratio for several values of parameter a. The flow non-uniformity index is defined as

$$\delta = \frac{100}{\overline{v}} \sqrt{\frac{\sum_{j=1}^{n} \varepsilon_j^2}{(n-1)}} (\%) \qquad (17)$$

where $\varepsilon_j = v_j - \overline{v}$, v_j is the area average velocity in the downstream channel j, $\overline{v}$ is the mean velocity over all downstream channels. CFD results clearly indicate that there is an optimum b/a ratio, which corresponds to a minimum of flow non-uniformity of 0.18–0.20%. In turn, the optimum ratio shifts to the higher b/a values by decreasing the distance between the downstream channels (*a*). Symbols in figure 9(*b*) show the optimum b/a ratios as a function of the distance between downstream channels. To investigate the effect of parameter c, three different geometries were studied at $a = 400$ μm. The numerical results were found to be in good agreement with the predictions obtained by equation (15). Figure 9(*c*) shows the safe operating range of b/a ratios in which the flow non-uniformity does not exceed 0.5%. The width of this range is rather constant (50 μm) for a distance a between 125 and 400 μm and then increases to 60 and 70 μm for a values of 500 and 750 μm, respectively. It should

be noted that the width of the safe range considerably exceeds the present precision of micromachining and assembling (about 10 μm).

Strategy to design the optimum geometry of a thick-walled screen

In many cases, the space between the downstream channels (*a*) and the height of the downstream channels (*d*) of a thick-walled screen are equal to the corresponding parameters $a1$ and $d1$ of the downstream microstructured reactor (figure 10(*a*)). In some cases to reduce the production costs, parameters a and d can be equal to the width of a group of reaction channels and the space between groups of reaction channels of the downstream microstructured reactor, respectively. A group of reaction channels can comprise e.g. two horizontal sets of reaction channels. In this particular example, a is equal to $a1$, while $d = 2d1 + a1$ (figure 10(*b*)). Such a design will decrease production costs without substantial deterioration of the flow non-uniformity. However in the latter case, very precise assembling of the microreactor relative to the downstream section of the screen is required, thereby causing an increase of the overall costs.

In the next step, parameters c, h and m of the upstream section have to be found. The first design criterion sets a limit on the number (*m*) of the upstream channels per 1 cm of length of the screen in the direction of the short edges of the upstream channels (*y*-direction, see figure 1). For the range of Re numbers of 0.5–10, eight parallel upstream channels are required per 1 cm of length for flow equalization [6]. The width of the upstream channels defines the degree of flow non-uniformity. For applications requiring a high degree of accuracy ($\delta < 0.2\%$, e.g. for screening of catalytic coatings),
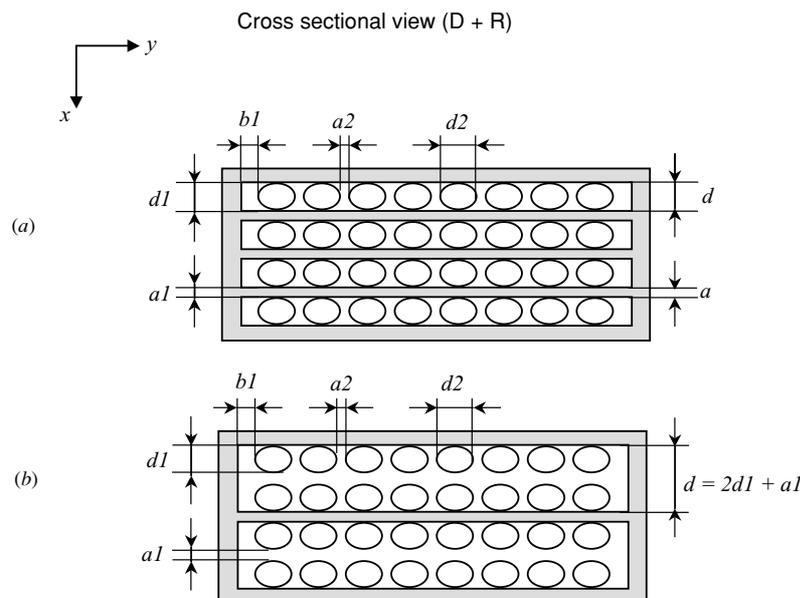
639

Cross sectional view (D + R)

Figure 10. Cross-sectional view (in the *xy* plane) of the interface between the downstream section (D) and the microstructured reactor (R). (*a*) Assembling scheme 1 to 1: one set of the downstream channels per one horizontal set of the reactor channels. (*b*) Assembling scheme 1 to 2: one set of the downstream channels per two horizontal sets of the reactor channels. See figure 1 for parameter definitions.

the recommended width of the upstream channels is between 200 and 300 μm. The width of the upstream channels of 500–800 μm is more acceptable for routine applications (e.g. a production microreactor), where a higher degree of flow non-uniformity (0.3–0.5%) is still acceptable. The sum of parameters *c* and *h* has to be 1260 μm.

To eliminate the dependence on the fluid velocity, the length of the upstream section (l_{up}) has to be 15 times larger than their width. However, if a small dead volume is a substantial requirement for the system, the upstream channel length can be decreased to a value as short as the spacing between two neighboring channels (*h*). The lower limit of l_{up} is defined by the definition of a thick-walled screen having a thickness of the separating bars in the direction of the fluid flow larger than the spacing between them. These sections can also be effectively used for the preheating of a fluid mixture. In the latter case, the overall length ($l_{up} + l_{dwn}$) is defined by the minimum distance required for warming up the mixture. This length can be calculated based on well-known engineering correlations [15]. In the next step, parameter *b* can be calculated by equation (15).

A similar approach can be applied to estimate parameter *b*1, which is the distance in the *xy* cross-sectional view between a side wall of the downstream channels and a wall of the first reactor channel (see figure 10). In the case of rectangular reactor channels, the problem of flow distribution at the D/R interface (figure 2(*d*)) becomes similar to that at the U/D interface (figure 2(*a*)). Therefore, analogous to the approach described above, parameter *b*1 can be calculated by equation (15), in which parameters *a*, *c*, *d* and x_{up}^+ are substituted by *a*2, *d*, *d*2 and x_{dwn}^+, respectively. Here $x_{dwn}^+ = \frac{l_{dwn}}{D_h Re}$ is the dimensionless length of downstream channels. This approach [6] can also be extended for other geometries of the microchannels (circular, oval, trapezoid, etc) to calculate the dependence of parameter P2 on the design parameters of the microstructured reactor.

Table 5. Average velocities in the downstream channels measured by LDA. The screen design parameter: $a = 0.3$ mm, $b = 0.29$ mm, $c = 0.86$ mm, $d = 2.26$ mm, $h = 0.3$ mm, $m = 8$, $n = 4$, $l_{up} = 10$ mm, $l_{dwn} = 40$ mm.

| Channel | Average velocity (mm s^{-1}) | | | |
	$Re = 6.7$	$Re = 12.7$	$Re = 64$	$Re = 113$
1	0.66 ± 0.01	1.16 ± 0.01	5.94 ± 0.02	9.76 ± 0.03
2	0.65 ± 0.01	1.19 ± 0.01	5.93 ± 0.02	9.86 ± 0.03
3	0.67 ± 0.01	1.15 ± 0.01	5.83 ± 0.02	9.83 ± 0.03
4	0.67 ± 0.01	1.16 ± 0.01	5.76 ± 0.02	9.78 ± 0.03
5	0.67 ± 0.01	1.16 ± 0.01	5.68 ± 0.02	9.49 ± 0.03
6	0.65 ± 0.01	1.15 ± 0.01	5.84 ± 0.02	9.71 ± 0.03
7	0.66 ± 0.01	1.19 ± 0.01	5.98 ± 0.02	9.75 ± 0.03
8	0.67 ± 0.01	1.18 ± 0.01	5.86 ± 0.02	9.49 ± 0.03

The dimensionless length of the screen channel (x_{up}^+) is a function of the *Re* number. However, if the length of the screen channel is much longer than its hydraulic diameter, the third term in equation (15) becomes rather small. For example, at x_{up}^+ of 5.0, the sum of the second and the third terms becomes 0.1683·*c*. Furthermore, if parameter *d* is substantially larger than parameter *c*, the fourth term in equation (15) is always much smaller compared to the first and second ones and, therefore, can be omitted. As a result, the optimum *b/a* value can be found by a simplified equation:

$$\frac{b}{a} = 0.5 + 0.1683\frac{c}{a}. \qquad (18)$$

Table 5 shows that a flow non-uniformity below 2% was obtained with the values of parameter *b* obtained by equation (18). One can see that no systematic trend is observed in the deviations between maximum velocities at the various *Re* numbers. The higher values of flow non-uniformities are caused by small (<3%) fluctuations in the flow rate within one experimental run, rather than by the deviation from the optimum *b/a* ratio.

Conclusions

The residence time distribution in the channels of a microstructured device determines the performance of the device. A systematic approach is proposed to design a thick-walled screen that can be positioned upstream of microstructured devices having constraints related to flow uniformity and pressure drop. The effect of the separation between the downstream channels (a), the minimum length between the top wall of the topmost downstream channel and a side wall of the upstream channels (b), the width of the upstream channels (c), the height of the downstream channels (d) and the dimensionless length of the channels (x^+) on the flow non-uniformity in the downstream channels of a thick-walled screen was established. The approximate solution corresponding to the minimum flow non-uniformity below 0.2% can be found by minimizing the difference between the volumetric flow in the first and the second downstream channels. A strategy to design the optimum geometry for a thick-walled screen is proposed, using a functional dependence of parameter b on the design parameters of the downstream microstructured reactor.

Acknowledgments

References

[1] Mueller A C and Chiou J P 1988 Review of various types of flow maldistribution in heat exchangers *Heat Transfer Eng.* **9** 36–50

[2] London A L 1970 Laminar flow gas turbine regenerators—the influence of manufacturing tolerances *J. Eng. Power* **92** 46–56

[3] Delsman E R, Uju C U, de Croon M H J M, Kramer G J and Schouten J C 2005 The influence of differences between micropassages on microreactor performance *Chem. Eng. Tech.* **28** 367–75

[4] Riman I S 1960 Modification of velocity profiles in variable cross section ducts by placement of meshes *Indust. Aerodyn.* **20** 216–38

[5] Taylor G I and Batchelor G K 1949 The effect of wire gauze on small disturbances in a uniform stream *J. Mech. Appl. Math.* **11** 1–29

[6] Rebrov E V, Ismagilov I Z, Ekatpure R P, de Croon M H J M and Schouten J C 2007 Header design for flow equalization in microstructured reactors *AIChE J.* **53** 28–38

[7] Wößner G and Linder E 1976 Abgasreaktor, insbesondere für Brennkraftmaschinen *German Patent* DE 2428964 A1

[8] Gulden P 1976 Apparatus for distributing flowing media from one flow cross section to a flow section different therefrom *US Patent* 3996025

[9] Harder R E 1968 *US Patent* 3406947

[10] Schrenk W J, Shastri R K, Ayres R E and Gosen D J 1992 *US Patent* 5094788

[11] Wen J and Li Y 2004 Study of flow distribution and its improvement on the header of plate-fin heat exchanger *Cryogenics* **44** 823–31

[12] Li Y Z and Zhang Z 2003 CFD simulation on the inlet configuration of plate-fin heat exchangers *Cryogenics* **43** 673–8

[13] Mies M J M, Rebrov E V, de Croon M H J M, Schouten J C and Ismagilov I Z 2006 Inlet section for micro-reactor *Patent* PCT/NL/050074

[14] Mies M J M, Rebrov E V, de Croon M H J M and Schouten J C 2004 Design of a molybdenum high throughput micro-reactor for high temperature screening of catalytic coatings *Chem. Eng. J.* **101** 225–35

[15] Shah R K and London A L 1978 *Laminar Flow Forced Convection in Ducts* (New York: Academic)

[16] Mies M J M, Rebrov E V, Deutz L, Kleijn C R, de Croon M H J M and Schouten J C 2007 Experimental validation of the performance of a microreactor for the high-throughput screening of catalytic coatings *I&EC Res.* at press

[17] Ismagilov I Z *et al* 2007 Oxidation of organic compounds in a microstructured catalytic reactor *Chem. Eng. J.* submitted

[18] Mies M J M, Rebrov E V, Schiepers C J B U, de Croon M H J M and Schouten J C 2007 High throughput screening of Co-BEA and Co-ZSM-5 coatings in the ammoxidation of ethylene to acetonitrile in a microstructured reactor *Chem. Eng. Sci.* published on-line at http://dx.doi.org/10.1016/j.ces.2006.12.018